Role of Two Residues Proximal to the Active Site of Ubc9 in Substrate Recognition by the Ubc9·SUMO-1 Thiolester Complex†

Michael H. Tatham,‡ Yuan Chen,§ and Ronald T. Hay*,‡

Centre for Biomolecular Sciences, University of St. Andrews, North Haugh, St. Andrews, Fife KY16 9ST, Scotland, and Division of Immunology, Beckman Research Institute of the City of Hope, 1450 East Duarte Road, Duarte, California 91010

Received September 16, 2002; Revised Manuscript Received December 19, 2002

ABSTRACT: The small ubiquitin-like modifier SUMO-1 is covalently attached to lysine residues on target proteins by a specific conjugation pathway involving the E1 enzyme SAE1/SAE2 and the E2 enzyme Ubc9. In an ATP-dependent manner, the C-terminus of SUMO-1 forms consecutive thiolester bonds with cysteine residues in the SAE2 subunit and Ubc9, before the Ubc9·SUMO-1 thiolester complex catalyzes the formation of an isopeptide bond between SUMO-1 and the ϵ-amino group of the target lysine residue on the protein substrate. The SUMO-1 conjugation pathway bears many similarities with that of ubiquitin and other ubiquitin-like protein modifiers (Ubls), and because of its production of a singly conjugated substrate and the lack of absolute requirement *in vitro* for E3 enzymes, the SUMO-1/Ubc9 system is a good model for the analysis of protein conjugation pathways that share this basic chemistry. Here we describe methods of both steady-state and half-reaction kinetic analysis of Ubc9, and use these techniques to determine the role of two residues, Asp^{100} and Lys^{101} of Ubc9 which are not found in E2 enzymes from other protein conjugation pathways. These residues are found close to the active site Cys in the tertiary structure of Ubc9, and although they are shown to inhibit the transesterification reaction from SAE1/SAE2, they are important for substrate recognition in the context of the thiolester complex with SUMO-1.

The small ubiquitin-like modifier SUMO-1[1] (also known as PIC1, SMT3, GMP1, and Sentrin), like ubiquitin, is found in the cell either in a free unbound form or covalently linked to specific proteins. However, unlike the case for ubiquitin which is usually attached to target proteins in the form of a polyubiquitin chain and predisposes them for degradation by the proteasome (see ref *1* for a review), the attachment of SUMO-1 is usually in the form of a single copy per site, and does not have a common consequence. Modification of specific proteins with SUMO-1 is known to control subcellular and nuclear targeting, stability, and direct functional regulation (recently reviewed in refs *2*−*4*). Although the spectrum of target proteins and the subsequent consequences of SUMO-1 modification differ from that of ubiquitin and other ubiquitin-like modifiers (Ubls), different Ubls are conjugated by homologous enzymes, have similar conjugation chemistry, and share the same tertiary fold known as the ubiquitin superfold. All known Ubls are initially expressed as inactive precursor proteins that undergo a maturation process. Specific proteases (C-terminal hydrolases) cleave inhibitory peptides from the C-terminal end of the inactive modifier to reveal a diglycine motif which is required for efficient catalysis by the conjugation machinery. The conjugation process can be broken down into three steps. In the first, a specific activating enzyme, E1 (SAE1/SAE2 for SUMO-1), forms an ATP-dependent adenylate intermediate with the Ubl before forming a high-energy thiolester bond between a conserved cysteine residue in E1 and the carboxyl group of the C-terminus of the modifier. In the second step, a transesterification reaction results in the transfer of thiolester from E1 to another cysteine residue on a specific E2 enzyme (Ubc9 for SUMO-1). The Ubl is then attached to the target protein via an isopeptide bond between the C-terminal carboxyl group of the modifier and the ϵ-amino group of a particular lysine reside on the substrate in the third step (see ref *5* for more details). For ubiquitin conjugation, this third step commonly requires an E3 ubiquitin-ligase protein (or complex). However, although E3-like proteins have been identified for the SUMO conjugation pathway (reviewed in ref *6*), they are not absolutely required for conjugation *in vitro*, because Ubc9 can itself bind specifically to substrates presenting a consensus SUMO modification motif, ψKxE (where ψ is typically a large hydrophobic residue, K the target lysine, x any residue, and E a glutamic acid). Structural analysis has recently revealed that this sequence is directly recognized by Ubc9 (*7*, *8*). Side

† Funded by the Medical Research Council (M.H.T. and R.T.H.) and NIH Grant GM59887 (Y.C.).

* To whom correspondence should be addressed. E-mail: rth@st-andrews.ac.uk.

‡ University of St. Andrews.

§ Beckman Research Institute of the City of Hope.

[1] Abbreviations: SUMO, small ubiquitin-like modifier; Ubl, ubiquitin-like modifier; E1, ubiquitin or Ubl activating enzyme; E2, ubiquitin or Ubl conjugating enzyme; E3, ubiquitin or Ubl ligase enzyme; SAE1/SAE2, SUMO activating enzyme subunits 1 and 2; Ubc, ubiqutin conjugating enzyme; Ubc9, SUMO conjugating enzyme; PML, promyelocytic leukemia protein; wt, wild-type.

10.1021/bi026861x CCC: $25.00
Published on Web 02/26/2003

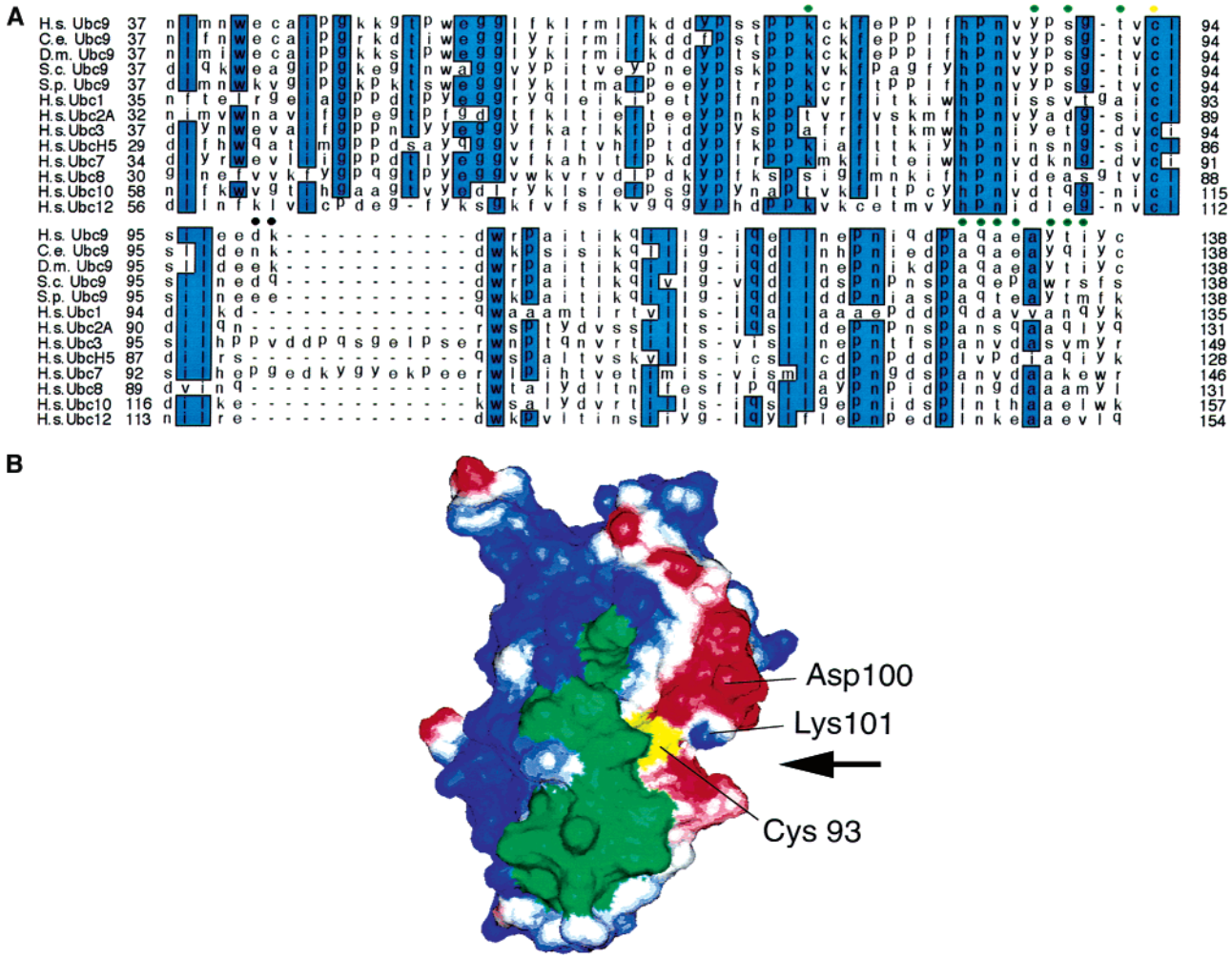

FIGURE 1: Unique two-residue insertion in the core domain close to the active site cysteine 93 in the Ubc9 tertiary structure. (A) Primary sequence comparison of the structurally conserved core domains of Ubc9 homologues from humans (H.s., *Homo sapiens*), nematodes (C.e., *Caenorhabditis elegans*), insects (D.m., *Drosophila melanogaster*), budding yeast (S.c., *S. cerevisae*), and fission yeast (S.p., *Schizosaccharomyces pombe*) (accession numbers P50550, NP_500604, AAC38964, NP_010219, and CAA91899, respectively) with human ubiquitin E2 enzymes (Ubc1, Ubc2A, Ubc3, UbcH5, Ubc7, Ubc8, and Ubc10) and the E2 for the Ubl NEDD8, Ubc12 (accession numbers P27924, P49459, P49427, CAA55019, BAA11410, XP_045947, O00762, and AAC26141). Identical residues are boxed and colored cyan. A yellow circle above the alignment indicates the position of the active site cysteine; green circles correspond to residues colored green in the structure in panel B, and black circles show the positions of Asp^{100} and Lys^{101} in the alignment. (B) Space-filling representation of Ubc9. Electrostatic potential is mapped to the surface where blue areas represent regions of net positive charge, red areas negative, and white areas neutrality. The green area is that shown by NMR (*8*) and crystallographic (*7*) studies to be important for target protein binding. Active site cysteine 93 is indicated and colored yellow, and aspartate 100 and lysine 101 are also indicated. The groove through which the C-terminal tail of SUMO-1 is proposed to pass when in a thiolester complex with Ubc9 (see the Discussion) is indicated with a black arrow.

chains from residues in the regions of residues 87−91 and 128−136 form a single contiguous surface adjacent to the active site Cys residue, and make direct contacts with substrate proteins in Ubc9−substrate noncovalent complexes (shown in Figure 1B in green).

As the SUMO-1 conjugation pathway shares its basic chemistry with those of ubiquitin and other Ubls, the relative simplicity of its *in vitro* analysis makes it an ideal model for furthering our understanding of the ubiquitin-like protein modification systems in general. E2 enzymes, which catalyze the conjugation of Ubl to substrate proteins, are likely to form direct interactions with substrate proteins and hence confer substrate specificity. Each E2 enzyme of the ubiquitin and homologous pathways is involved in the conjugation of a unique subset of substrate proteins. However, how different E2 proteins with their high degrees of sequence and structural similarity confer specificity for their particular pathways is poorly understood. Sequence alignments of E2 enzymes reveal that differences in size mostly exist as nonconserved N- and C-terminal extensions, which are generally thought to be the predominant determinants of E2 specificity (*9*, *10*). However, within the ~140-amino acid conserved central core domain, some E2 enzymes contain loop insertions near the active site in the three-dimensional structures. To understand the function of this insertion in the SUMO-specific E2 Ubc9, the corresponding residues (Asp^{100} and Lys^{101}) were mutated to Ala. Here we describe in detail the use of *in vitro* assays and kinetic studies which allow detailed analysis of the mechanism of Ubc9-catalyzed steps in the SUMO-1 conjugation pathway. These studies revealed that Asp^{100} and more significantly Lys^{101} affect Ubc9 catalysis both positively and negatively at different points in the Ubc9 catalytic mechanism. In fact they inhibit the transfer of SUMO-1 from SAE1/SAE2, but are important for efficient transfer of SUMO-1 onto target proteins. Kinetic analysis revealed that the residues are important for target protein binding, by reducing

the association rate and increasing the dissociation rate of the Ubc9·SUMO-1∼target protein complex. These results show that Asp^{100} and more significantly Lys^{101} play an important role in Ubc9 substrate binding in the context of the SUMO-1·Ubc9 thiolester complex.

MATERIALS AND METHODS

cDNA Cloning. Mutants of Ubc9 encoding the single and double substitutions of amino acids Asp^{100} and Lys^{101} with Ala were generated using two-stage PCRs. All mutants were PCR amplified using the external primers 5′-ACAAACGGATCCATGTCGGGGATCGCCCTCAGC-3′ and 5′-GCCGCGGAATTCTTATGAGGGCGCAAACTTC-TTGGC-3′. Each mutant was PCR amplified using the following internal primers: 5′-CCTCCAGTCCGCGGC-CTCCTCTAA-3′ and 5′-TTAGAGGAGGCCGCGGACTG-GAGG-3′ for D100A/K101A-Ubc9, 5′-CCAGTCCTTGGC-CTCCTCTAA-3′ and 5′-TTAGAGGAGGCCAAGGACTGG-3′ for D100A-Ubc9, and 5′-CCTCCAGTCCGCGTCCT-CCTC-3′ and 5′-GAGGAGGACGCGGACTGGAGG-3′ for K101A-Ubc9. The external primers facilitate cloning of PCR products into pGEX-2T using the restriction enzymes *Bam*HI and *Eco*RI. All DNA constructs were verified by automated DNA sequencing on an ABI PRISM 377 DNA sequencer (St. Andrews University DNA Sequencing Unit).

Expression and Purification of Recombinant Proteins. Recombinant SAE2/SAE1, GST-PML, wt-Ubc9, wt-SUMO-1, and C52A-SUMO-1 were expressed and purified as described previously (*8*, *11*). Mutants of Ubc9 were expressed and purified in the same manner as the wild type (wt), except Q130A, E132A, and Y134A variants, which were prepared as described previously (*8*). All recombinant protein identities were confirmed by MALDITOF mass spectrometry (St. Andrews University Mass Spectrometry Unit), and concentrations were determined using Bradford's method (*12*).

In Vitro Conjugation Assays Using ^{35}S-Labeled Protein Substrates. An *in vitro* conjugation assay was used for preliminary analysis of the effects of the different Ubc9 mutations on their ability to conjugate SUMO-1 to [^{35}S]-methionine-labeled protein substrates. ^{35}S-labeled full-length p53, IκBα, and PML (promyelocytic leukemia protein) proteins were generated using an *in vitro* wheat germ-coupled transcription/translation system as described previously (*11*). Each Ubc9 protein was incubated at 1.1 μM in a 10 μL reaction mixture with 0.11 μM recombinant SAE1/SAE2, in 50 mM Tris (pH 7.5), 5 mM $MgCl_2$, 2 mM ATP, 10 mM creatine phosphate, 3.5 units/mL creatine kinase, 0.6 unit/mL IPP, 8.9 μM SUMO-1, and 1 μL of ^{35}S-labeled substrate. Reaction mixtures were incubated at 37 °C for 2 h (IκBα and p53) or 1 h (PML) such that approximately equal proportions of each substrate were conjugated to SUMO-1 by wt-Ubc9 over these incubation periods. Reactions were terminated by addition of SDS sample buffer containing β-mercaptoethanol, and the mixtures were fractionated on 8 to 10% polyacrylamide gels containing SDS, which were stained and destained before drying and analysis by phosphorimaging (Fujix MacBas software, version 2.5).

Prior experiments had shown that under these assay conditions the extent of accumulation of the SUMO-conjugated product was proportional to both the concentration of Ubc9 and the incubation time over the stated periods (data not shown). Assays were performed in triplicate, and the percentage of the substrate conjugated by SUMO was determined by quantitative analysis (MacBas software) of phosphorimage results.

SUMO-1 Thiolester Transfer Assays from SAE1/SAE2 to Ubc9. To determine the effect of the Ubc9 mutants on the E1 to E2, SUMO-1 transfer step, assays that monitor the rate of the transesterification reaction of ^{125}I-labeled SUMO-1 from SAE1/SAE2 to Ubc9 were employed. First, 0.29 μM SAE1/SAE2·SUMO-1 thiolester complex was formed by incubation at 37 °C for 60 min of a reaction mixture containing 6.9 mM ATP, 0.14 unit/μL IPP, 17.4 mM $MgCl_2$, 138.9 mM Tris-HCl (pH 7.5), 0.51 μM SAE2/SAE1, and 2.46 μM [^{125}I]SUMO-1. To halt the reaction, EDTA was added to a final concentration of 50 mM which inhibits further ATP-dependent thiolester formation. Samples (4 μL) were taken after EDTA addition to represent "zero" time points, and were added to 4 M urea sample buffer in the absence of a reducing agent. Because of the speed of the SAE1/SAE2 to Ubc9 transfer step, all assay solutions and equipment were then cooled to 4 °C before addition of Ubc9, to slow the reaction progress. Time course reactions were started by addition of the SAE2·SUMO-1 complex to a solution of Ubc9 in a 1:1.5 ratio, thus diluting the SAE2·SUMO-1 complex to 0.115 μM, with a final Ubc9 concentration of 0.31 μM. Reactions (10 μL) were terminated after 10, 20, 30, and 60 s by addition of 4 M urea sample buffer in the absence of a reducing agent. Reaction products were fractionated on polyacrylamide gels containing SDS and gels processed as described above. Radioactive species were detected and quantitated by phosphorimaging.

Recombinant C52A-SUMO-1 was radiolabeled with ^{125}I using the chloramine-T method as described previously (*11*). The mutant form was used instead of the wild-type protein to avoid experimental complications from SUMO-1·SUMO-1 disulfide-linked dimers.

SUMO-1 Transfer Assays for Transfer from Ubc9 to GST-PML. To examine the second step of Ubc9 catalysis (substrate binding and isopeptide bond formation), preformed [^{125}I]SUMO-1·Ubc9 thiolester complexes were added to the recombinant substrate and the formation of [^{125}I]SUMO-1−substrate conjugates was assessed over time.

[^{125}I]SUMO-1·Ubc9 thiolesters were formed in 3.3 mM ATP, 8.3 mM $MgCl_2$, 67 mM Tris-HCl (pH 7.5), and 67 units/mL IPP in the presence of 0.24 μM SAE1/SAE2, 2.36 μM [^{125}I]C52A-SUMO-1, and 3.3 μM (each) Ubc9 protein sample. Reaction mixtures were incubated for 30 min (wt, Q130A, E132A, and Y134A), or for 13, 20, and 13 min (D100A/K101A, D100A, and K101A, respectively) at 37 °C to accumulate approximately equal quantities of SUMO-1·Ubc9 thiolesters (0.38−0.55 μM), before addition of EDTA to a concentration of 20 mM. Transfer reactions were started by addition of 27 μL of the batch mix containing the thiolester complexes to a 7 μL solution containing GST-PML (schematically shown in Figure 3A, and characterized in ref *8*) to give a final concentration of 5 μM. Reaction mixtures were incubated at 37 °C and samples taken after 5, 15, and 30 min, and the reactions were halted by addition to 4 M urea/SDS sample buffer lacking a reducing agent. Reaction products were fractionated by SDS−PAGE and

analyzed by phosphorimaging as described above. Quantitative analysis of phosphorimage results allowed the calculation of the concentration of the newly formed GST-PML−SUMO-1 complex for each time point and Ubc9 variant.

For half-reaction kinetic analysis of the Ubc9 to substrate SUMO-1 transfer step, the final concentration of GST-PML used to initiate reactions was varied from 0.5 to 30 μM (as indicated in Figure 6), and hence, the rate of transfer from Ubc9 to GST-PML was monitored over a range of substrate concentrations.

Conjugation of [^{125}I]SUMO-1 to GST-PML for Steady-State Kinetic Analysis of Ubc9 Mutants. GST-PML at 1, 2, 5, 10, 20, and 30 μM was used in 10 μL conjugation assays with 1.43 μM (each) Ubc9 protein, 6.44 μM [^{125}I]C52A-SUMO-1, and 0.11 μM SAE2/SAE1, in the presence of 2.0 mM ATP, 5.0 mM $MgCl_2$, 50 mM Tris-HCl (pH 7.5), and 0.6 unit/mL IPP. Assays were incubated for 60 min at 37 °C before being stopped by the addition of SDS sample buffer containing β-mercaptoethanol. Reaction products were then fractionated by SDS−PAGE and analyzed as described above. Under these conditions, the ATP regeneration system and SUMO-1 maintain an excess of the E1−SUMO-1 thiolester over Ubc9, and thus, a pseudo-steady-state reaction is produced (herein simply termed steady state).

Under these conditions, wt-Ubc9 was seen to be rate-limiting to the reaction, and the extent of accumulation of SUMO-conjugated GST-PML was proportional to incubation time over the period of 60 min (data not shown). Assays were performed in triplicate, and the concentration of newly formed GST-PML−SUMO-1 conjugates was determined by quantitative analysis of phosphorimaging results. Initial reaction rates (v_0) could then be calculated and used to extrapolate steady-state kinetic information for each Ubc9 mutant over a range of substrate concentrations.

RESULTS

Asp^{100} and Lys^{101} Mutants of Ubc9 Have Impaired Overall Conjugation Activity. Sequence alignments of the core regions of E2 enzymes reveal the existence in some proteins of nonconserved insertions from 2 to 13 amino acids in length, 6 residues downstream from the active site cysteine. Figure 1A shows an alignment of the core UBC domains of Ubc9 homologues from humans, nematodes, fruit-flies, budding yeast, and fission yeast, with a number of human ubiquitin-specific E2 enzymes, Ubc1, Ubc2A, Ubc3, UbcH5, Ubc7, Ubc8, Ubc10, and Ubc12 (the human E2 enzyme for the Ubl NEDD8). In human Ubc9, the insertion corresponds to residues Asp^{100} and Lys^{101} which in the tertiary fold of the protein are close to the active site cysteine (see Figure 1B), but are of unknown function. To determine whether Asp^{100} and Lys^{101} are important for the overall conjugation activity of Ubc9, *in vitro* SUMO-1 conjugation assays were used to compare wt-Ubc9 with three mutants, D100A/K101A (DK-AA), D100A, and K101A. In these reactions, rate-limiting quantities of Ubc9 conjugate SUMO-1 onto ^{35}S-labeled, full-length, protein substrates. Assays were incubated at 37 °C for periods over which the conjugation of SUMO-1 to all substrates was known to be proportional to time for the wt-Ubc9 protein. As such, under these conditions, the extent of accumulation of SUMO-1-modified substrates directly relates to the initial rate of the Ubc9 conjugation reaction. Reaction products were separated by SDS−PAGE and analyzed by phosphorimaging. Single examples of raw data from triplicate reactions for wt and the mutants of Ubc9, comparing their conjugation activity using p53, PML, and IκBα as substrates, are shown in Figure 2A−C. Quantitative analysis of the data indicates that the double mutation of both Asp^{100} and Lys^{101} to Ala has significantly affected the overall conjugation activity of Ubc9 in these assays for all substrates that have been tested, reducing the initial rate of overall catalysis by ~2.5-fold for each substrate. The mutation of Lys^{101} to Ala caused a 1.7−1.4-fold reduction in activity, while the mutation of Asp^{100} to Ala had a weaker effect, varying from undetectable to a 1.3-fold reduction

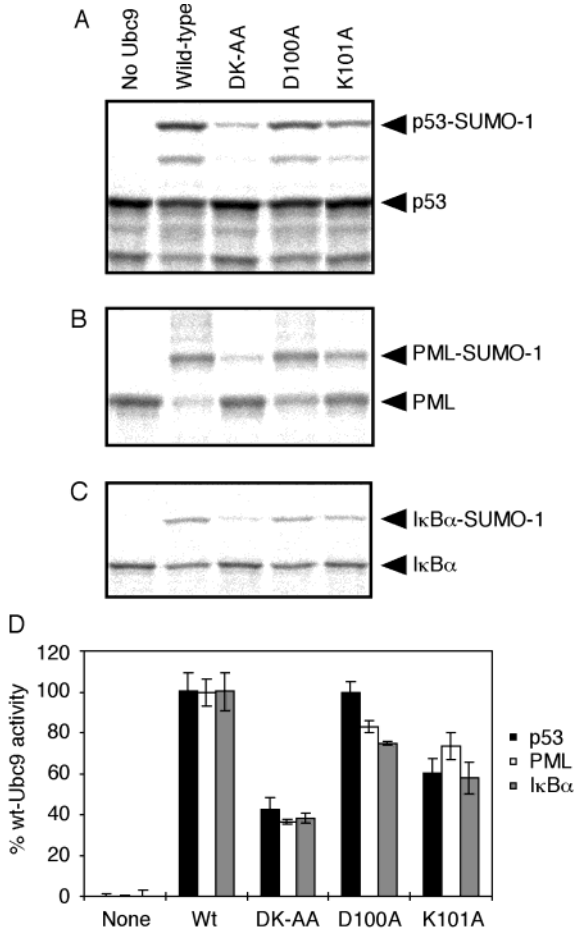

FIGURE 2: Ubc9 mutants of Asp^{100} and Lys^{101} are defective in overall SUMO-1 conjugation. Rate-limiting concentrations of Ubc9 wt, D100A/K101A, D100A, and K101A were incubated in triplicate *in vitro* conjugation assays using ^{35}S-labeled PML, p53, and IκBα as substrates as described in Materials and Methods. Under these conditions, the level of production of the SUMO-1-modified substrate was known to be linear with respect to time for the incubation periods. Reactions were terminated with SDS sample buffer before fractionation on 8 to 10% polyacrylamide gels containing SDS. Gels were stained, destained, and dried before analysis by phosphorimaging. Examples of raw phosphorimage data from a single reaction of each triplicate condition using p53, PML, and IκBα as substrates are shown in panels A−C, respectively. Quantitative analysis of radioactive species (Mac Bas software) allowed calculation of the percent SUMO-1-conjugated substrate for each condition. Using no Ubc9 and wt-Ubc9 as 0 and 100% standards, respectively, the percent conjugation values for each condition were determined (D). Columns represent mean percent conjugation values and error bars one standard deviation from the mean as calculated from triplicate reactions.

Scheme 1: Two Steps of Ubc9 Catalysis[a]

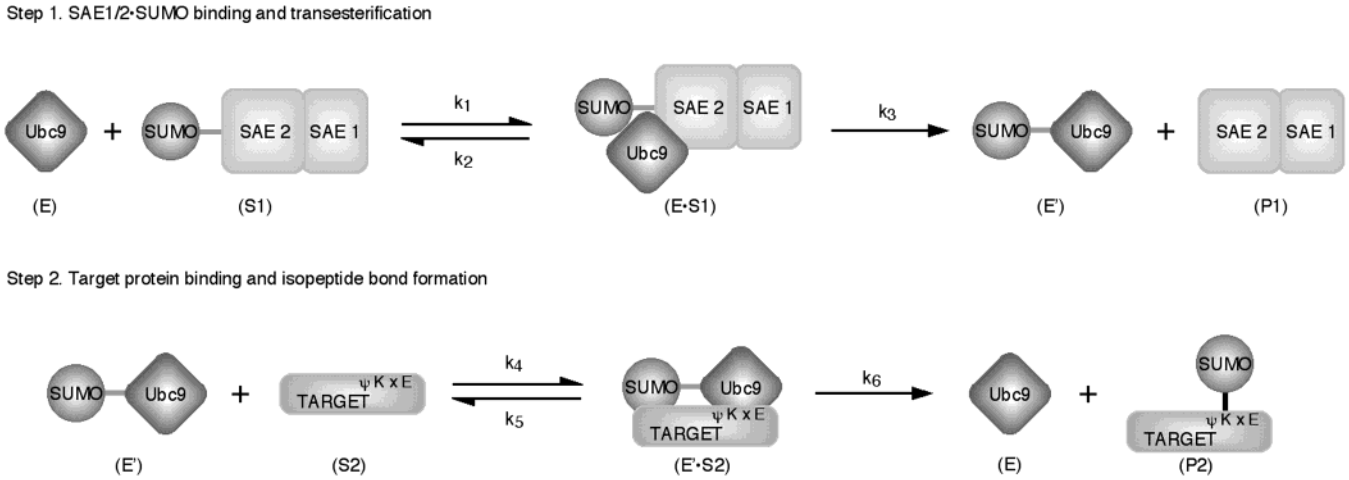

[a] In the role of Ubc9 as the E2 enzyme of the SUMO-1 conjugation pathway, its mechanism of catalysis can be divided into two steps, during which it converts two substrates into two products. In the first (top half), Ubc9 (E) binds the SAE1/SAE2·SUMO-1 thiolester complex (S1), forming an enzyme·substrate complex (E·S), followed by a transesterification reaction whereby the SUMO-1 thiolester bond (shown as a gray line) is transferred from a cysteine residue on the SAE2 subunit onto cysteine 93 in the Ubc9 active site. This results in the formation of the modified enzyme form, Ubc9·SUMO-1 thiolester (E′), and the release of first product, SAE1/SAE2 (P1). The association and dissociation rate constants (k_{on} and k_{off}) for the Ubc9∼SAE1/SAE2·SUMO complex are shown as k_1 and k_2, respectively, while the catalytic rate constant (k_{cat}) for the first step is shown as k_3. In the second step (bottom half), this Ubc9·SUMO-1 thiolester (E′) then recognizes and binds to the specific protein target (S2) and catalyzes the formation of an isopeptide bond (shown as a black line) between the C-terminal carboxyl group of SUMO-1 and the ϵ-amino group of the specific lysine residue. This generates a target−SUMO-1 conjugate (P2) and regenerates the free enzyme, Ubc9. In almost all cases, this lysine is found within the SUMO-1 conjugation consensus motif, ψKxE (where ψ represents a large hydrophobic residue, K the target lysine, x any residue, and E a glutamic acid group). The association and dissociation rate constants for the target∼Ubc9·SUMO complex are shown as k_4 and k_5, respectively, while the catalytic rate constant for the first step is shown as k_6.

(Figure 2D). In general, the double mutant appears to have the cumulative defects of the two single mutants in this assay. However, although this analysis shows that the mutations introduced into Ubc9 reduce the level of SUMO conjugation, it does not identify the step(s) in the SUMO-1 conjugation pathway affected by the amino acid substitutions.

Mutants of Asp[100] and Lys[101] positively affect SUMO-1 transfer from SAE1/SAE2 but negatively affect transfer of SUMO-1 to substrates.

Ubc9 catalysis can be broken down into two steps or half-reactions (as shown in Scheme 1). In the first, Ubc9 binds the SAE1/SAE2·SUMO-1 thiolester complex and the thiolester bond is transesterified from the putative active site Cys[173] of SAE2 onto Cys[93] of Ubc9. The second step involves the Ubc9·SUMO-1 thiolester binding to the target substrate, followed by formation of an isopeptide bond between the C-terminus of SUMO-1 and the specific lysine residue within the ψKxE motif of the target substrate. This two-step catalysis means that any mutations which affect the overall catalytic activity of Ubc9 can, in principle, affect either step or both steps of the pathway. To clarify which of the two steps is affected by the mutants, two transfer assays were employed which monitor, over time, the transfer of radiolabeled SUMO-1 from SAE1/SAE2 onto Ubc9, and from Ubc9 onto a recombinant target substrate.

To study the E1 to E2 step, the transfer of ^{125}I-labeled SUMO-1 from SAE1/SAE2 onto Ubc9 was analyzed over 60 s at 4 °C (see Materials and Methods for further details). Phosphorimaging results with assay reaction products fractionated by SDS−PAGE are shown in Figure 3A. The data show that under these conditions the mutants of Ubc9 transesterify SUMO-1 from SAE1/SAE2 at a faster rate than wt. This is most significant in the double mutation of Asp[100] and Lys[101] to Ala, and it is Lys[101] which has the greater influence. Quantitative analysis of radioactive species allowed the determination of the percentage of SUMO-1 transferred from SAE1/SAE2 onto each Ubc9 type (Figure 3B). Analysis of the initial rates of these reactions suggests that the E1 to E2 transfer reaction involving the double mutant of Ubc9 progresses at a rate approximately 5 times that of the wt protein.

The E2 to substrate transfer assay analyzes the rate of [^{125}I]SUMO-1 transfer from Ubc9 onto a recombinant substrate, GST-PML. GST-PML is a previously characterized artificial SUMO-1 substrate (*11*) composed of the 11 amino acids containing one of the conjugation sites of PML ([485]PRKVI**K**MEESEE[495]), fused to GST (Figure 3C, bottom). Ubc9·SUMO-1 thiolester complexes were generated for each of the Ubc9 mutants, and after addition of GST-PML (5 μM), the transfer to substrate was monitored over 30 min at 37 °C. In contrast to the E1 to E2 transfer data, phosphorimage results (Figure 3C) show that the rate of transfer of SUMO-1 from Ubc9 to GST-PML is slower for the mutants. Again, the double mutant has the largest defect, which is almost entirely due to the Lys[101] mutation as the mutant of Asp[100] has little effect on this step. The percentage of SUMO-1 transferred, shown in Figure 3D, shows that under the conditions of this assay the E2 to substrate transfer step is approximately 2.5 times faster for wt-Ubc9 than for the double mutant when considering initial rates.

Asp[100] and Lys[101] Are Involved in Substrate Recognition. The Ubc9 residues Asp[100], and to a greater extent Lys[101], appear to reduce the efficiency of the transesterification reaction from SAE1/SAE2, but are required for efficient transfer of SUMO-1 onto target proteins. However, on the basis of the above data and the proximity of the two residues to the active site, it is not possible to discriminate between an effect on catalysis or target protein binding interactions.

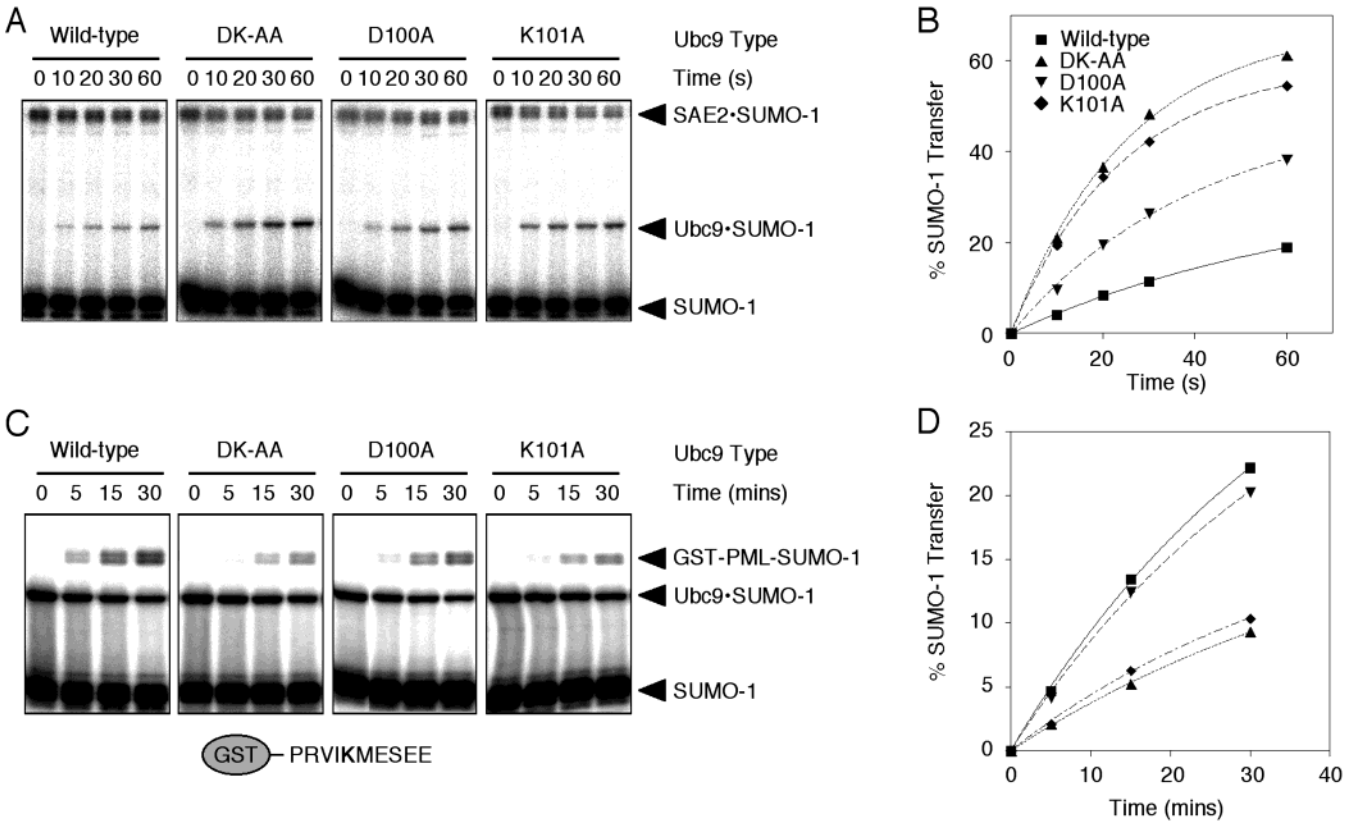

FIGURE 3: Mutation of Asp[100] and Lys[101] in Ubc9 increases the rate of transfer of SUMO-1 from SAE1/SAE2, but reduces the rate of transfer from GST-PML. Ubc9 mutants of Asp[100] and Lys[101] were compared with wt for their rate of transfer of SUMO-1 from SAE1/SAE2 (A and B) and from themselves onto a recombinant substrate, GST-PML (C and D). For E1 to E2 transfer assays, thiolester complexes of [^{125}I]SUMO-1 and SAE1/SAE2 were formed by incubation at 37 °C for 1 h, in a reaction mixture containing the two proteins, ATP, $MgCl_2$, IPP, and buffer (pH 7.5) (as described in detail in Materials and Methods). Formation of the thiolester complex was halted by the addition of EDTA. Later analysis revealed the concentration of the SAE1/SAE2·SUMO-1 thiolester to be 115 nM in the final assays. All solutions and equipment were cooled to 4 °C before initiation of the transfer reaction by addition of Ubc9 to a concentration 0.31 μM. At 10, 20, 30, and 60 s postinitiation, 10 μL samples were taken and reactions halted by addition of 4 M urea/SDS sample buffer in the absence of a reducing agent. For E2 to substrate transfer assays, first thiolester complexes were formed between [^{125}I]SUMO-1 and wt, D100A/K101A (DK-AA), D100A, and K101A in separate reactions similar to those described above for the E1 thiolester adducts, but including 3.3 μM Ubc9 (see Materials and Methods for details). Again further formation was stopped by addition of excess EDTA, and later analysis showed the concentration of Ubc9·SUMO-1 complexes to be between 0.388 and 0.55 μM for all Ubc9 types in the final reaction mixtures. Transfer reactions were initiated at 37 °C, by addition of samples of each Ubc9·SUMO-1 thiolester mix to a solution of the recombinant substrate protein GST-PML (see the bottom of panel C for a schematic representation) up to a final substrate concentration of 5 μM. Samples (10 μL) were removed 5, 15, and 30 min after initiation, which were halted by addition of 4 M urea/SDS sample buffer in the absence of a reducing agent. For both types of assay, samples were fractionated by SDS−polyacrylamide gel electrophoresis, and radioactive species were detected from dried gels by phosphorimaging. Panels A and C show raw phosphorimaging data of the transfer reactions for each Ubc9 construct (as indicated above the gel images). Free [^{125}I]SUMO-1 and the conjugated complexes with Ubc9, SAE2, and GST-PML are shown. Quantitative analysis allowed the determination of the absolute quantities of each radioactive species and hence the calculation of the percent SUMO-1 transferred from SAE2 or Ubc9. This is represented graphically in panels B and C. "Zero" time points were taken prior to transfer initiation.

Experiments were therefore designed to allow kinetic analysis to distinguish between these two possibilities.

The catalytic reaction of the E2 enzyme Ubc9 is a compulsory-order, substituted-enzyme, or ping-pong Bi Bi mechanism. As the SAE1/SAE2 to Ubc9 transesterification of SUMO-1 can occur in the absence of a target substrate (as shown in Figure 3), Ubc9 catalysis fits the definition of a ping-pong mechanism, and thus, the ternary complex model can be excluded. As such, Ubc9 catalysis can be broken down as follows. The enzyme, E (Ubc9), is first modified by one substrate, S1 (SAE1/SAE2·SUMO-1 thiolester), to form the modified enzyme, E′ (Ubc9·SUMO-1 thiolester), and release the first product, P1 (SAE1/SAE2). The modified enzyme, E′, then interacts with the second substrate, S2 (target protein), to form the final product, P2 (target−SUMO-1 conjugate), and yield the free enzyme again. This mechanism is also shown in Scheme 1, and can be summarized as

$$\mathrm{E} + \mathrm{S1} \underset{k_2}{\overset{k_1}{\rightleftharpoons}} \mathrm{E{\cdot}S1} \xrightarrow{k_3} \mathrm{P1} + \mathrm{E'}$$

$$\mathrm{E} + \mathrm{S2} \underset{k_5}{\overset{k_4}{\rightleftharpoons}} \mathrm{E{\cdot}S2} \xrightarrow{k_6} \mathrm{P2} + \mathrm{E'} \qquad (1)$$

To evaluate whether the amino acid substitutions affected the binding of protein substrates to the E2−SUMO-1 thiolester (k_4 and k_5) or the catalytic rate constant (k_6) of the transfer reaction, the kinetics of the second half-reaction were examined for each Ubc9 construct. In these experiments, SUMO-1·Ubc9 thiolester complexes were formed in a separate reaction first (to make between 0.35 and 0.5 μM in the final assays), then different concentrations of the GST-

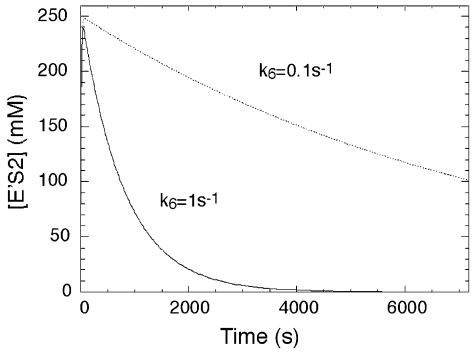

FIGURE 4: Calculated concentrations of the Ubc9·SUMO-1∼substrate intermediate over time based on a numerical integration using the Runge−Kutta method show steady-state kinetic parameters are not appropriate for transfer assay analysis. Equations 2−5 (see the Results) were used in a simulation described by the Runge−Kutta method (*32*) to calculate the concentration of the Ubc9·SUMO-1∼substrate complex (E′S2) concentration in a reaction where Ubc9·SUMO-1 thiolester conjugates transfer SUMO-1 to a protein substrate. The kinetic constants used for the simulation are as follows: $k_4 = 1 \times 10^6\ M^{-1}\ s^{-1}$, $k_5 = 0.1\ s^{-1}$, and two different k_6 values (the solid line corresponds to a k_6 of $1\ s^{-1}$ and the dotted line to a k_6 of $0.1\ s^{-1}$). Nonhorizontal traces for the two simulations demonstrate that the E′S2 concentration does not reach steady state in the transfer reactions.

PML target proteins were added, and the transfer of SUMO-1 from Ubc9 to the protein substrate was monitored over time. The reaction mechanism isolated in this assay is summarized by the second step of eq 1. The rate equations can be mathematically described in detail as follows:

$$\frac{d[E'\cdot S2]}{dt} = k_4[E'][S2] - k_5[E'\cdot S2] - k_6[E'\cdot S2] \quad (2)$$

$$\frac{d[P2]}{dt} = k_6[E'\cdot S2] \quad (3)$$

$$[E'] = [E']_0 - x;\ [S2] = [S2]_0 - x \quad (4)$$

$$[P2] = x - [E'\cdot S2] \quad (5)$$

where $[E']_0$ and $[S2]_0$ are the initial concentrations of Ubc9·SUMO-1 thiolester and the target protein, GST-PML, respectively. Equations 4 and 5 state that the SUMO-1 protein is transferred from E2 to the target protein and the total amount of SUMO-1 protein in different states does not change. In this reaction mechanism, the amount of Ubc9·SUMO-1 thiolester (which can be regarded as the "active enzyme") is being consumed, and not recycled; therefore, the "steady state" of the enzyme−substrate intermediate does not exist. This is shown in a simulation of the changes of the concentration of the enzyme−substrate intermediate (E′·S2 in eq 1) over time as shown in Figure 4. If this is the case, then the rate of change of the E′·S2 complex concentration over time (left part of eq 2) is not equal to zero, and therefore, the data produced by this type of half-reaction analysis cannot be analyzed by steady-state enzyme kinetic approaches. Equations 2 and 3 are coupled differential equations that can be solved using numerical integration approaches.

To extract kinetic information from the second step of the Ubc9 catalytic mechanism, the Ubc9 to substrate, SUMO-1 transfer assay (described above) was performed using a range of GST-PML concentrations from 0.5 to 30 μM. Assays were performed and data processed as described above for each Ubc9 type at each of the seven GST-PML concentrations. Quantitative analysis of phosphorimager results allowed the calculation of the concentrations of Ubc9·SUMO-1 thiolester and the GST-PML−SUMO-1 conjugate during the course of the transfer reaction. These kinetic data were fit to eqs 2−5 by numerical integration using the software KINSIM and FITSIM (*13*), and the fits of the simulated curves to experimental data for wt, D100A/K101A, D100A, and K101A Ubc9 protein samples are shown in Figure 5A−D. Each curve corresponds to the transfer reactions at different substrate concentrations with the same starting concentration of the Ubc9·SUMO-1 thiolester complex. Values for the kinetic constants (k_4−k_6) were calculated for each Ubc9 type. The set of kinetic constants that gives the best fit to transfer data of wt-Ubc9 is given in Table 1, and the fit is shown in Figure 5A. These kinetic constants were also calculated for the SUMO-1 transfer data of the three mutant Ubc9 proteins. For the K101A substitution, three calculations were performed by keeping one of the kinetic constants (k_4, k_5, or k_6) the same as that of wt-Ubc9 and optimizing the fit to experimental data by adjusting the other two kinetic constants. This approach was used to limit the degrees of freedom in the data fitting. The kinetic constants that best fit the data are given in Table 1, and the fit between the calculated curves and the experimental data is shown in Figure 5D. These calculations suggest that the k_4 (k_{on}) value is the most significantly affected kinetic constant. k_4 is reduced ∼2.4-fold by the amino acid substitution, while k_5 (k_{off}) was calculated to be the same as that of wt and k_6 (k_{cat}) ∼25% higher. The transfer kinetic data for the D100A substitution fit the kinetic constants of wt-Ubc9 well, which indicates that Asp^{100} does not have a significant role in the transfer of SUMO-1 from Ubc9 to the target protein. Further optimization of the fit shows that only k_{off} increased slightly relative to that of the wt protein (Table 1), and the fit is shown in Figure 5C. The double substitution of both D100 and K101 with Ala has a more significant effect on the kinetics of the transfer reaction than either mutant alone, and in fact shows some synergism above the cumulative effect of the two individual mutations. The kinetic constants that best fit the transfer data indicate that the most significant effect of the double mutation is to reduce the on rate and increase the off rate of the substrate and, therefore, reduce the affinity of the substrate for the Ubc9·SUMO thiolester. As with the K101A mutant, the double mutant also appears to slightly increase k_{cat}, which suggests that this substitution may have a small, positive effect on the rate of formation of the isopeptide bond between SUMO-1 and GST-PML after the complex between the Ubc9·SUMO-1 thiolester and GST-PML (E·S2) has formed.

To confirm the validity of this half-reaction analysis method and to compare these mutants with some known to disrupt direct target binding, three other Ubc9 mutants characterized in a previous study were analyzed. NMR chemical shift perturbations of a region from residue 126 to 135 of Ubc9 were detected upon formation of a complex with peptide fragments of target proteins (*8*). Of these residues, Gln^{130} and Tyr^{134} were shown by steady-state kinetic analysis to be important for target binding, while Glu^{132} was shown not to play a significant role. The wild type and the

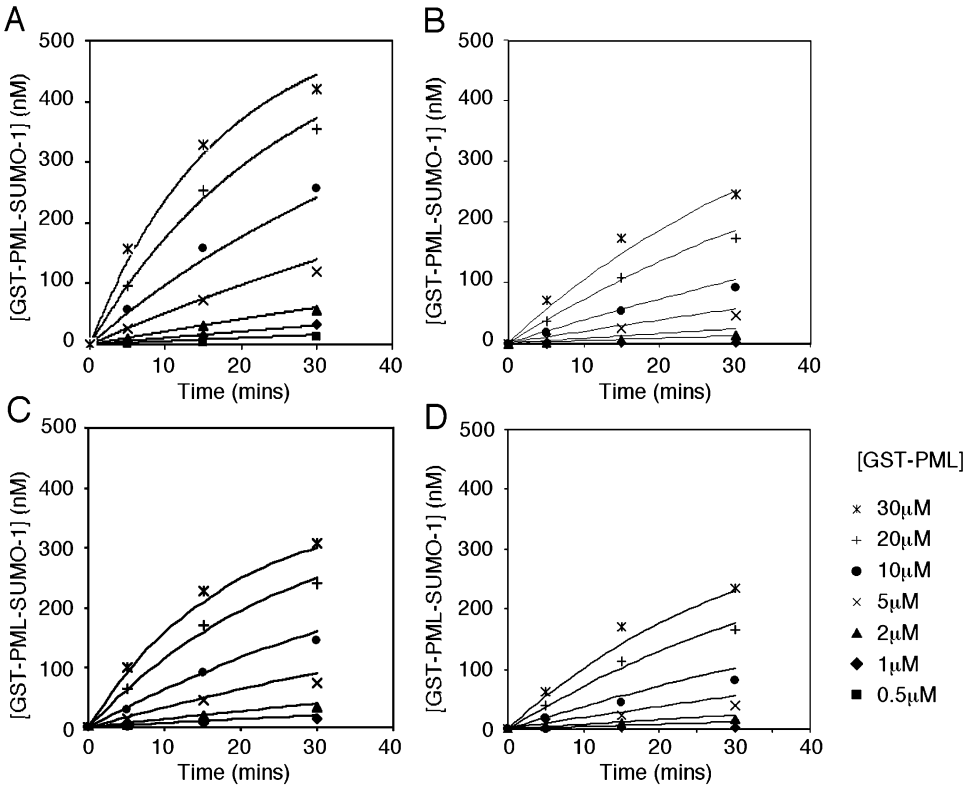

FIGURE 5: Transfer assay data fit well to the half-reaction kinetic model. E2 to GST-PML transfer reactions were prepared in a manner identical to that described in the legend of Figure 3, with the exception that a range of GST-PML concentrations from 0.5 to 30 μM (as indicated) was used to initiate the transfer. Reactions were processed and analyzed as described in the legend of Figure 3, and quantitative analysis of GST-PML and Ubc9 thiolester-conjugated SUMO-1 species allowed determination of their concentrations in the reaction mixtures. The fitting of these data to the kinetic model for the transfer reaction (see eqs 2 and 3) can be seen for wt (A), D100A/K101A (DK-AA) (B), D100A (C), and K101A (D) Ubc9 proteins. The lines show calculated transfer kinetic curves at different substrate concentrations, and the points are the experimentally measured amount of product at the indicated time points. Data for the 0.5 μM set have been omitted for the Ubc9 mutants as they were below the sensitive range of the assay.

Table 1: Kinetic Constants Obtained from Half-Reaction Studies and Numerical Integration

Ubc9	k_4 or k_{on} (M^{-1} min^{-1})	k_5 or k_{off} (min^{-1})	k_6 or k_{cat} (min^{-1})
wild type	2.7×10^6	2197	1.6
D100A/K100A	1.04×10^6	2625	2.0
D100A	2.7×10^6	2246	1.6
K101A	1.14×10^6	2197	2.0
Q130A	0.81×10^6	2141	1.6
E132A	3.4×10^6	2226	1.6
Y134A	0.99×10^6	2263	1.6

mutants Q130A, E132A, and Y134A of Ubc9 were analyzed by the half-reaction kinetic analysis method as described above, again using GST-PML as a target protein. The experimental data were fit to eqs 2−5 using KINSIM/FITSIM as described above (data not shown), and the resultant values of k_4-k_6 for the mutants are shown in Table 1. The data for wt-Ubc9 were consistent with the prior experiment (not shown), and for Q130A and Y134A, the mutants of the two residues known to be involved in substrate binding, there are 3.2- and 2.6-fold reductions in the rate of Ubc9 binding to GST-PML. E132A-Ubc9 actually has a slightly higher k_4 value, consistent with the mildly positive phenotype of this mutant shown previously. For each of these substrate binding site mutants, the k_5 and k_6 values are largely unchanged from those of the wt protein, indicating that the effect of the substitutions in Ubc9 is on the association event with GST-PML. In comparison, it can be seen that the effect on affinity for the target protein of Q130A and Y134A mutations is similar to that of K101A, showing that Lys^{101}, Glu^{130}, and Tyr^{134} are equally significant for the target protein binding event.

Under the conditions of the E1 to E2 transfer assay, the SAE1/SAE2·SUMO-1 thiolester can be regarded as the active enzyme of the system, Ubc9 as the substrate, and the Ubc9·SUMO-1 thiolester and free SAE1/SAE2 as the products. Therefore, in theory, by varying the concentration of the Ubc9 and monitoring the rate of product formation, we should be able to determine the kinetic constants for the process by applying the data to a model for the mechanism. Unfortunately, the resultant data could not be applied to any of the proposed models of transfer kinetics, implying that this SAE1/SAE2 binding and transesterification step of Ubc9 catalysis does not conform to this simple scheme.

Steady-State Kinetic Analysis of Asp^{100} and Lys^{101} Ubc9 Mutants Confirms the Conclusions of the Half-Reaction Kinetic Analysis. Although, as discussed above, steady-state kinetic approaches are not appropriate for the analysis of the half-reactions of Ubc9 catalysis, they have previously been used to effectively analyze the overall reactions of ubiquitin-specific E2 and E3 enzymes (*14*, *15*). As mentioned above, this method has also recently been used to determine the effect site-directed mutants of Ubc9 had on substrate binding, again using overall (both half-reactions) conjugation assays (*8*). To verify in general the conclusions from the half-reaction kinetic analysis, previously established steady-

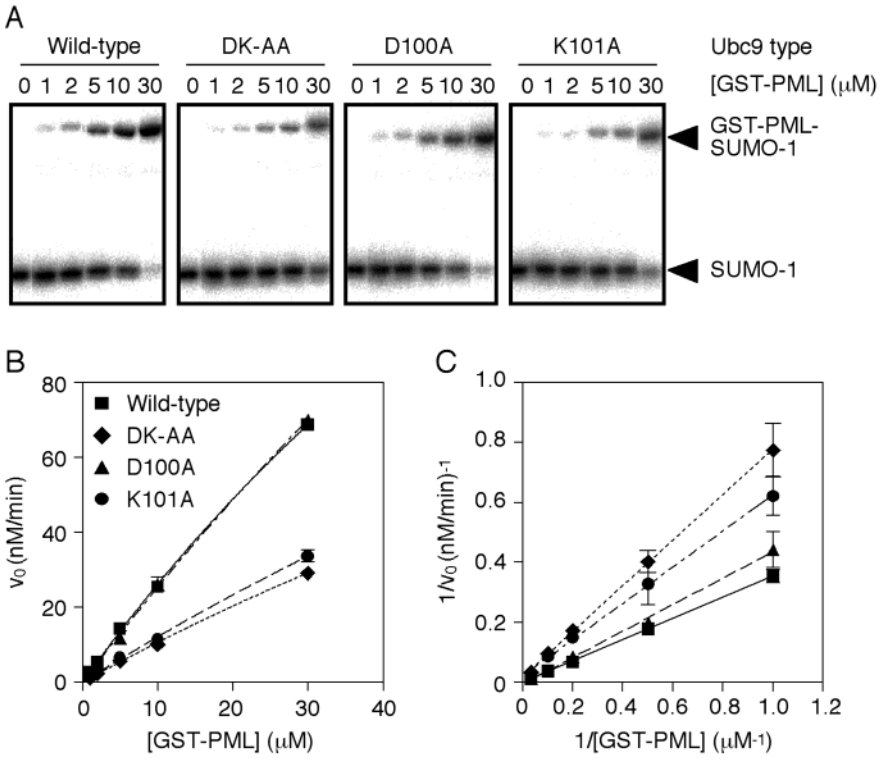

FIGURE 6: Confirmation of the kinetic properties of the Ubc9 mutants by steady-state kinetic analysis. Conjugation reaction mixtures using rate-limiting quantities of Ubc9 were incubated in triplicate for periods known to be within the linear range of SUMO-1 conjugation with respect to time. Reactions conjugate ^{125}I-labeled SUMO-1 to the recombinant substrate GST-PML at varying concentrations from 0 to 30 μM (as indicated; see Materials and Methods for details of the assay composition). Reactions were halted by addition to SDS sample buffer, and the mixtures were fractionated on polyacrylamide gels containing SDS. Gels were stained and destained before drying and analysis by phosphorimaging. Part A shows results of samples of the triplicate data for each Ubc9 construct at each GST-PML concentration, and data for both conjugated and unconjugated SUMO-1 species are shown. Quantitative analysis of radioactive species allows the calculation of the concentration of each SUMO-1 species in the assays, and hence the initial rates (v_0) for each Ubc9 construct at each GST-PML concentration. The mean values and standard deviations were calculated and expressed graphically in v_0 vs [GST-PML] and double-reciprocal plots of $1/v_0$ vs 1/[GST-PML] (B and C, respectively).

state kinetic analysis was employed (see ref *8* for further details). In steady-state kinetic experiments, the ping-pong Bi Bi mechanism can be described as (*16*)

$$\frac{e}{v_0} = \phi_0 + \frac{\phi_1}{[S1]} + \frac{\phi_2}{[S2]} \quad (6)$$

where e is the total enzyme (Ubc9 in this case) concentration and $\phi_0-\phi_2$ are given by

$$\phi_0 = \frac{1}{k_3} + \frac{1}{k_6}$$

$$\phi_1 = \frac{k_2 + k_3}{k_1 k_3}$$

$$\phi_2 = \frac{k_5 + k_6}{k_4 k_6} \quad (7)$$

The double-reciprocal plot of $1/v_0$ versus the inverse of either substrate concentration should be linear and the slope of the plot proportional to ϕ_1 or ϕ_2. Thus, steady-state kinetic analysis with a varying target substrate (S2) concentration would also allow dissection of the roles of Asp^{100} and Lys^{101} in Ubc9 catalysis by determining comparative values of ϕ_2.

Steady-state kinetic experiments using wt and mutant Ubc9 proteins were carried out using the same substrate protein as for the half-reaction analysis, GST-PML, and [^{125}I]SUMO-1 as the modifier (as described in Materials and Methods). Conjugation reactions were performed with limiting Ubc9 concentrations and over periods where the extent of product formation was known to be proportional to time (data not shown) so that initial rates (v_0) of the overall conjugation reaction could be calculated. The steady-state kinetic parameters extracted from these data thus reflect only the kinetic properties of the Ubc9 protein under analysis. Assays were processed in the same manner as described for the transfer assays described above, and phosphorimaging analysis detected both the GST-PML-conjugated and unconjugated SUMO-1. Figure 6A shows examples of single reactions from triplicate assays of GST-PML conjugated to [^{125}I]SUMO-1 by the different Ubc9 protein samples as indicated. Quantitative analysis of the data allowed the calculation of mean v_0 values at each GST-PML concentration (as indicated), and estimation of uncertainties in the measurements of the calculated slopes of double-reciprocal plots. These data are presented a plot of v_0 versus GST-PML concentration and a double-reciprocal plot of $1/v_0$ versus 1/concentration in panels B and C of Figure 6, respectively.

The double-reciprocal plots are linear, which verifies that eq 6 is appropriate for the description of the reaction mechanism, and as Ubc9 catalysis is a ping-pong Bi Bi

Table 2: Comparison of Kinetic Parameters Obtained from Steady-State and Half-Reaction Kinetic Analysis

Ubc9	ϕ_2 values calculated from double-reciprocal plots (μM min)	ϕ_2 values calculated from kinetic constants (μM min)
wild type	515 ± 43	509
D100A/K101A	1187 ± 43	1256
D100A	543 ± 29	520
K101A	1073 ± 86	965

mechanism, these data can be used to isolate the effects of the mutants for the second step of its catalytic mechanism (transfer of SUMO-1 from Ubc9 to substrate). This is because the slope of the double-reciprocal plot of $1/v_0$ versus the inverse of the target protein concentration ($1/s$) is proportional to ϕ_2 as described in eq 7. This only relates to the second half-reaction, the lower part of eq 1, and under steady-state conditions is independent of any effects in the first step, the transfer of SUMO-1 from SAE1/SAE2 to Ubc9. In fact, the slope values are equivalent to ϕ_2/e, where ϕ_2 is the inverse of the observed rate constant of SUMO-1 being transferred from E2 to GST-PML and e is the concentration of Ubc9. Visual comparison of the plots shown in Figure 6C indicates that mutation of Asp^{100} and, more significantly, Lys^{101} results in slopes that are steeper than wt slopes and, hence, decrease the rate of transfer of SUMO-1 from Ubc9 to the substrate. Also, consistent with prior analysis, the double mutation of Asp^{100} to Ala and Lys^{101} to Ala appears to have the cumulative defect of the two single mutants individually. Identical experiments using GST-p53 (GST fused to KKLMF**K**-TEGPD) and GST-IκBα (GST fused to PRDGL**K**KERLL) as substrate proteins gave results very similar to those for GST-PML, suggesting that the mutants do not have substrate-specific effects.

The results of the steady-state kinetic analysis are in very close agreement with the half-reaction kinetic analysis. The two sets of data can be compared directly via the constant ϕ_2. As mentioned earlier, the slope of the double-reciprocal plots of the steady-state data (Figure 6C) is equal to ϕ_2/e, and therefore, multiplication of the slope values by Ubc9 concentration gives the value of ϕ_2. The ϕ_2 values calculated from the kinetic constants that were extracted from the numerical integration of half-reaction kinetic data are also given in Table 2. Clearly, the two ϕ_2 values determined by the steady-state and half-reaction experiments are similar, and the differences between them are within the error range of the experimental procedures and quantitative analysis. The comparison further verifies the results of the numerical integration calculation of the half-reaction experiments. With respect to the functional mutants, the two methods together suggest that significantly Lys^{101} and to a lesser extent Asp^{100} are important for interactions with the target proteins.

The kinetic constants of K_m and V_{max} cannot be reliably determined from this analysis because of the low affinity of Ubc9 for GST-PML. Thus, levels of substrate protein concentration approaching saturation cannot be achieved, and only data for the very early, almost linear portion of the v_0 versus s graph can be collected. This produces large errors in V_{max} calculations from linear regression analysis and graphical manipulations of the double-reciprocal data. These effects are probably due to the lack of a specific E3 ligase for the reaction.

DISCUSSION

In ubiquitin conjugation pathways, substrate specificity is determined by a combination of E2 and E3 enzymes. It is likely that E2 forms direct interactions with target proteins in most of these modification processes, and directly contributes to substrate specificity. The relatively conserved core region of E2 enzymes (see Figure 1A for a selection) consists of ~140 amino acids, which in all published E2 enzyme structures forms a common tertiary fold known as the UBC domain. Within this conserved core domain, some E2 enzymes contain sequences of amino acids which appear as insertions of varying length within the primary sequence relative to the consensus. Human Ubc9 has one such insertion of only two residues, aspartate 100 and lysine 101, whose side chain termini are only approximately 8 and 5 Å, respectively, from cysteine 93 in the active site (*17*, *18*). Two residue insertions are also found at the same sequence position in other Ubc9 homologues, although the side groups are not strictly conserved (see the alignment in Figure 1A). To investigate whether this invariant region is important for the specific functions of Ubc9 in the SUMO conjugation pathway, *in vitro* functional analysis of site-directed mutants was employed. Analysis of Ubc9 mutants of aspartate 100 and lysine 101 showed that both residues are important for overall conjugation, and further analysis revealed that it is the E2 to target protein transfer step which is negatively affected. The *in vitro* Ubc9 to target protein transfer assay was modified to monitor the rate of transfer of SUMO-1 from Ubc9 onto the recombinant GST-PML substrate at varying concentrations. These data were then fit using KINSIM and FITSIM to the equations describing the kinetic rate constants of this half-reaction (eqs 2−5 and Scheme 1). As such, the association and dissociation rate constants of the Ubc9·SUMO-1~GST-PML complex and the catalytic rate constant for the formation of the covalently modified GST-PML (k_4-k_6 from eq 1, respectively) were calculated for wt-Ubc9 and the mutants. This revealed that lysine 101, and to a lesser degree aspartate 100, are important for protein substrate binding. For the double mutant of (both Asp^{100} and Lys^{101} changed to Ala), this results from an ~2.5-fold decrease in the association rate in combination with a slight increase (~25%) in the dissociation rate. This half-reaction analysis method was also used to determine which of these catalytic rate constants were affected by mutation of three side chain groups shown in a previous study to be involved in target protein binding (*8*). This showed that the mutations had little or no effect on the dissociation or catalytic rate constants, but lowered the rate of association of Ubc9 with the target protein by between 2.7- and 3.3-fold. Clearly, the 2.5-fold reduction caused by mutation of Lys^{101} suggests that this residue plays a role in substrate binding just as important as that of either Gln^{130} or Tyr^{134}. The already established technique of steady-state kinetic analysis was used to both qualitatively and quantitatively confirm the general conclusions of the half-reaction analysis, demonstrating the consistency of this method with current techniques.

The fact that Lys^{101} is shown to be important for substrate recognition is unexpected as both NMR (*8*) and crystallographic (*7*) studies of Ubc9 in complex with protein substrate fragments do not show any direct interactions between this residue and the bound target proteins. These

two studies independently mapped the substrate binding site to the same face of Ubc9 as lysine 101, but the opposite side of the active site (green in Figure 1B). However, under conditions of SUMO-1 conjugation, it is the Ubc9·SUMO-1 thiolester adduct which binds substrates and transfers SUMO-1 onto target lysine residues, and as such, it is in the context of the Ubc9·SUMO-1 thiolester that lysine 101 appears to be important for substrate recognition. The simplest explanation for this is that, by being in a thiolester complex with SUMO-1, Ubc9 may bind target proteins in a manner slightly different from that of Ubc9 alone. However, functional analysis of Ubc9 mutants shows that residues identified by these studies of Ubc9 in a non-thiolester complex with target proteins are important for conjugation activity (*7*, *8*). Thus, a shift in the substrate binding site in the context of a Ubc9·SUMO-1 thiolester seems to be unlikely.

Because of the instability of the thiolester bond, to date the structure of an E2 enzyme in a thiolester complex with its specific Ubl has not been directly determined. However, a model of the catalytic domain of a Ubc1 from *Saccharomyces cerevisiae* in the thiolester complex with ubiquitin based on regions of interaction identified by NMR experiments during *in situ* thiolester formation has recently been published (*19*). In this E2·ubiquitin thiolester model, ubiquitin interacts with Ubc1 on the face opposite from that shown to be important for substrate binding in Ubc9 (hidden side of the protein as shown in Figure 1B). The C-terminal tail of ubiquitin (residues 71−76) is thought to position itself in a shallow cleft that locates the terminal glycine in a position with the active site cysteine residue of Ubc1. If such an interaction is conserved in all E2·Ubl thiolester complexes, then the cleft that accommodates the C-terminus of SUMO-1 (indicated with a black arrow in Figure 1B) is formed by Ser^{95}, Glu^{98}, Asp^{102}, Asp^{124}, Asn^{127}, and Lys^{101}. A model of Ubc9 in a thiolester complex with SUMO-1 (not shown) based on the Ubc1·ubiquitin structure shows that the C-terminus of SUMO-1 forms a contiguous surface with Ubc9 in the region known to be important for substrate recognition, suggesting that elements from the C-terminus of SUMO-1 may also play a role in substrate binding. If this is the case, then a possible explanation for the observed phenotypes of mutants of aspartate 100 and lysine 101 from Ubc9 may be that they alter the substrate binding properties of the Ubc9·SUMO-1 thiolester by failing to orient the C-terminus of SUMO-1 in a manner conducive to optimal protein binding.

Interestingly, although the mutations of Asp^{100} and Lys^{101} had negative effects on the substrate recognition step of Ubc9 catalysis, they actually enhanced the rate of the transesterification reaction from SAE1/SAE2. Basic analysis shows that the double mutant is approximately 5 times as fast as wt-Ubc9 in forming Ubc9·SUMO-1 thiolester complexes under the conditions described here. The fact that the phenotype of the mutants in overall conjugation reactions (as shown in Figures 2 and 6) is inhibitory is due to the Ubc9 to target protein transfer step and not the SAE1/SAE2 to Ubc9 step, being the rate-limiting process of the pathway. Although an explanation for the increased rate of the SAE1/SAE2 to Ubc9 half-reaction could be that Asp^{100} and Lys^{101} interfere with Ubc9 binding SAE1/SAE2, it is more likely that the two side groups represent a local physical barrier to the transesterification reaction and hence impede the transfer of SUMO from SAE1/SAE2 to Ubc9. More to this point, in both Ubc9 constructs with Lys^{101} mutated, the catalytic rate constant for the GST-PML−SUMO-1 conjugate formation (k_6 in eq 1) is ~25% higher than that of wt. This could also be due to lysine 101 acting as an impediment to the efficient transfer of SUMO-1 from Ubc9 onto the target protein. The proposed role of these residues simply as a steric hindrance to SUMO C-terminal mobility during Ubc9 catalysis may also explain why the side chains are not conserved throughout different species other than as bulky groups which could still fulfill this role.

Attempts to determine the precise role of Asp^{100} and Lys^{101} in the SAE1/SAE2 to Ubc9·SUMO-1 transfer process using modeling analysis similar to that applied to the Ubc9 to substrate transfer reaction were unsuccessful. This mechanism is in fact not as simple as expected, an observation which appears to be consistent for different E1 enzymes. A recent steady-state kinetic analysis of the ubiquitin E1 enzyme (*20*) revealed that in the presence of excess ubiquitin and ATP, the increase in reaction velocity does not follow a simple hyperbolic relationship with the concentration of E2 (Ubc4) as would be expected if Michaelis−Menten kinetics applied. In fact, although the reaction rate initially increases with Ubc4 concentration up to ~2 μM, higher levels are inhibitory. Wee and co-workers suggest that substrate inhibition by Ubc4 may best explain these observations, and fit their data for ubiquitin E1 catalysis to a simple substrate inhibition model (*20*). We have used the same approach to analyze the SUMO E1 enzyme (not shown), and although a similar substrate inhibition is seen after approximately 1 μM Ubc9, the extent of this inhibition does not increase at higher concentrations. At Ubc9 concentrations of >3 μM, the effect reverts back from inhibition of reaction velocity to stimulation. Wee and co-workers only assayed up to 10 μM Ubc4, and the data in the range of proposed substrate inhibition do not appear to fit to a simple substrate inhibition model well (*20*), suggesting that it is possible that the reactivation of E1 catalysis at high E2 enzyme concentrations may also be conserved for ubiquitin E1 catalysis, albeit to a lesser degree than for SAE1/SAE2. Due to the facts that SAE1/SAE2 can covalently modify itself with SUMO (M. H. Tatham and R. T. Hay, unpublished results), Ubc9 forms high-affinity noncovalent complexes with SUMO-1 in the absence of SAE1/SAE2 (*21*), and Ubc9 also appears to bind SAE1/SAE2 in the absence of SUMO-1 (*22*), kinetic analysis of reaction mixtures containing all these components is clearly not trivial. Without further extensive analysis of SAE1/SAE2 catalysis, the roles of mutated residues in this half-reaction in the SUMO-1 conjugation pathway cannot be thoroughly analyzed.

The observations described in detail here, that residues close to the active site of an E2 enzyme can play both positive and negative roles in catalysis, are consistent with a study showing that a variable loop near the active site of a ubiquitn-specific E2, Ubc7, is important in the transfer of ubiquitn to target proteins (*23*). Partial characterization of this loop in the rabbit homologue of Ubc7, known as $E2_{17K}$, indicated that it negatively influences the transfer of ubiquitin from E1, but plays an important role in substrate binding (*23*). The crystal stucture of yeast Ubc7 (*24*) shows the loop protruding from the core E2 domain spatially proximal to the active site Cys residue, and forming a deep groove in

the region equivalent to that shown in Ubc1 to accommodate the ubiquitin C-terminus in the thiolester model. While this loop is much larger in Ubc7 and Ubc3 than in Ubc9, these data are consistent with the hypothesis that insertions close to the active site are important for the interaction of the E2−thiolester complex with substrates.

Recently, it has been shown that selection of target proteins for modification by SUMO-1 is aided by a number of proteins that appear to function in a fashion similar to the specificity-determining E3s in the ubiquitin system (*25*−*31*). They share no apparent sequence homology with ubiquitin E3 ligases, but some contain the E2 binding motif known as the RING sequence, which is found in many ubiquitin-specific E3s. A possible role for the E3 enzymes could be to stabilize the Ubc9·SUMO-1∼substrate complex, and this should significantly reduce the off rate (k_5) of the reaction. Reduction of the off rate can significantly increase the rate constant of net transfer of SUMO-1 from Ubc9 to substrates. In this study, we have developed a half-reaction kinetic method that can be used to extract individual kinetic constants in the conjugation process. The ability to extract these values is an important tool for determining the effects of functional mutants of Ubc9 or additional factors (such as E3s) involved in the reaction. This study emphasizes the importance of both structural and functional analysis in the understanding of the catalytic mechanisms of enzymes from ubiquitin and other Ubl pathways, and identifies a novel method for further analysis of these systems.

ACKNOWLEDGMENT

We thank Dr. Roger Griffiths for help and advice regarding the design of kinetic experiments and Professors Carl Frieden for help with KINSIM and FITSIM and Timothy O'Connor and Shiuan Chen for helpful discussions. Many thanks to Dr. Rona Ramsay for critical review of the manuscript. We also thank Dr. Catherine Botting for mass spectrometry analysis of Ubc9 constructs, Mr. Alex Houston for DNA sequencing, and Mr. Ellis Jaffray for purified proteins.

REFERENCES

1. Pickart, C. M. (2000) *Trends Biochem. Sci. 25*, 544−548.
2. Muller, S., Hoege, C., Pyrowolakis, G., and Jentsch, S. (2001) *Nat. Rev. Mol. Cell Biol. 2*, 202−210.
3. Wilson, V. G., and Rangasamy, D. (2001) *Exp. Cell Res. 271*, 57−65.
4. Kim, K. I., Baek, S. H., and Chung, C. H. (2002) *J. Cell Physiol. 191*, 257−268.
5. Hochstrasser, M. (2000) *Nat. Cell Biol. 2*, E153−E157.
6. Hochstrasser, M. (2001) *Cell 107*, 5−8.
7. Bernier-Villamor, V., Sampson, D. A., Matunis, M. J., and Lima, C. D. (2002) *Cell 108*, 345−356.
8. Lin, D., Tatham, M. H., Yu, B., Kim, S., Hay, R. T., and Chen, Y. (2002) *J. Biol. Chem. 277*, 21740−21748.
9. Kolman, C. J., Toth, J., and Gonda, D. K. (1992) *EMBO J. 11*, 3081−3090.
10. Silver, E. T., Gwozd, T. J., Ptak, C., Goebl, M., and Ellison, M. J. (1992) *EMBO J. 11*, 3091−3098.
11. Tatham, M. H., Jaffray, E., Vaughan, O. A., Desterro, J. M., Botting, C. H., Naismith, J. H., and Hay, R. T. (2001) *J. Biol. Chem. 276*, 35368−35374.
12. Bradford, M. M. (1976) *Anal. Biochem. 72*, 248−254.
13. Dang, Q., and Frieden, C. (1997) *Trends Biochem. Sci. 22*, 317.
14. Baboshina, O. V., Crinelli, R., Siepmann, T. J., and Haas, A. L. (2001) *J. Biol. Chem. 276*, 39428−39437.
15. Hofmann, R. M., and Pickart, C. M. (2001) *J. Biol. Chem. 276*, 27936−27943.
16. Dalziel, K. (1957) *Acta Chem. Scand. 11*, 1707−1723.
17. Giraud, M. F., Desterro, J. M., and Naismith, J. H. (1998) *Acta Crystallogr. D54*, 891−898.
18. Tong, H., Hateboer, G., Perrakis, A., Bernards, R., and Sixma, T. K. (1997) *J. Biol. Chem. 272*, 21381−21387.
19. Hamilton, K. S., Ellison, M. J., Barber, K. R., Williams, R. S., Huzil, J. T., McKenna, S., Ptak, C., Glover, M., and Shaw, G. S. (2001) *Structure 9*, 897−904.
20. Wee, K. E., Lai, Z., Auger, K. R., Ma, J., Horiuchi, K. Y., Dowling, R. L., Dougherty, C. S., Corman, J. I., Wynn, R., and Copeland, R. A. (2000) *J. Protein Chem. 19*, 489−498.
21. Liu, Q., Jin, C., Liao, X., Shen, Z., Chen, D. J., and Chen, Y. (1999) *J. Biol. Chem. 274*, 16979−16987.
22. Bencsath, K. P., Podgorski, M. S., Pagala, V. R., Slaughter, C. A., and Schulman, B. A. (2002) *J. Biol. Chem. 277*, 47938−47945.
23. Lin, H., and Wing, S. S. (1999) *J. Biol. Chem. 274*, 14685−14691.
24. Cook, W. J., Martin, P. D., Edwards, B. F., Yamazaki, R. K., and Chau, V. (1997) *Biochemistry 36*, 1621−1627.
25. Sachdev, S., Bruhn, L., Sieber, H., Pichler, A., Melchior, F., and Grosschedl, R. (2001) *Genes Dev. 15*, 3088−3103.
26. Johnson, E. S., and Gupta, A. A. (2001) *Cell 106*, 735−744.
27. Kotaja, N., Karvonen, U., Janne, O. A., and Palvimo, J. J. (2002) *Mol. Cell. Biol. 22*, 5222−5234.
28. Pichler, A., Gast, A., Seeler, J. S., Dejean, A., and Melchior, F. (2002) *Cell 108*, 109−120.
29. Takahashi, Y., Toh-e, A., and Kikuchi, Y. (2001) *Gene 275*, 223−231.
30. Azuma, Y., and Dasso, M. (2002) *Dev. Cell 2*, 130−131.
31. Kahyo, T., Nishida, T., and Yasuda, H. (2001) *Mol. Cell 8*, 713−718.
32. Press, W. H., Flannery, B. P., Teukolsky, S. A., and Vetterling, W. T. (1989) *Numerical Recipes*, Cambridge University Press, Cambridge, U.K.

BI026861X